Path Generation for Foam Additive Manufacturing of Large Parts with a Cable-Driven Parallel Robot

Elodie Paquet, Marceau Metillon, Kevin Subrin, Benoit Furet, Stéphane Caro

Path Generation for Foam Additive Manufacturing of Large Parts with a Cable-Driven Parallel Robot

Elodie PAQUET[1], Marceau METILLON[1], Kevin SUBRIN[1], Benoit FURET[1] and Stéphane CARO[1]

[1] Nantes Université, Ecole Centrale Nantes, CNRS, LS2N, UMR 6004, F-44000 Nantes, France

elodie.paquet@ls2n.fr, marceau.metillon@ls2n.fr, kevin.subrin@ls2n.fr, benoit.furet@ls2n.fr, stephane.caro@ls2n.fr

Abstract -

In this paper, a framework for foam printing with a Cable-Driven Parallel Robot (CDPR) is described for building large parts. Compared with the traditional robotic systems, CDPRs have a large workspace that can include the printing area. In addition, the potential reconfigurability of CDPRs is an asset to get rid of the collisions between the cables and the environment during the execution of the printing task. The printing feasibility is verified through the process identification where key parameters are used in the proposed control law. The features to be taken into account through a framework to make a successful printing with a CDPR are described. Finally, advantages and drawbacks of CDPRs for additive manufacturing are discussed and future work is presented.

Keywords -

Additive Manufacturing; Cable-Driven Parallel Robot; Innovative Construction

Figure 1. Additive foam manufacturing: BatiPrint3D, Yhnova's house 3D Printing with an AGV and a serial robot

1 Introduction

3D printing solutions are generally based on Cartesian robots with a 2D motion in the horizontal plane and a 1D motion for the support table, corresponding to a three degrees of freedom machines [1][2][3]. For printing large parts, several materials can be used such as: plastic materials [5], polymer foams [1][4][5] concrete [2][6][7], or materials based on metallic particles [8][9]. The combination of automatic system and process has allowed multiple advances for large-scale 3D-printing, particularly house walls in construction fields. For instance, BatiPrint3D™ construction technology, composed of a Staubli poly-articulated arm and a B2A Systems Automatic Guided Vehicle (AGV), was proposed by Nantes University, France (Figure 1). In 2017, Yhnova demonstrator became a 95m^2 social dwelling built for the social landlord Nantes Métropole Habitat (NMH) [4].

The 3D-printing demonstrator BatiPrint3D™ technology focuses on the construction of house walls through the deposition of two layers of polymer foam used as a formwork for a third concrete layer inside. To build large parts without interruption in the printing process that would be related to the concatenation of the different workspaces of a mobile robot, the use of CDPRs for additive manufacturing in a short term is conceivable [7][10][11][12]. CDPRs are a potentially suitable replacement for very large-scale applications [8][13]. They easily achieve a large workspace without requiring massive equipment and machinery [14, 15].

This paper introduces a framework to adapt the 3D Printing process to a CDPR. A printing head with polymer foam for the production of large parts is managed by this architecture. The 3D foam printer performance is demonstrated through the construction of two different large parts, with an accuracy equal to 1 cm. The advantages and drawbacks of the novel 3D printer are then discussed. The paper is organized as follows: Section 2 introduces the process and the robotic architecture and a way to identify key parameters to adapt the process on a CDPR. Section 3 highlights the experimental validation and proposes a framework to fulfill the need. Section 4 draws some conclusions and future work.

2 Spraying End-Effector mounted on a CDPR

2.1 Spraying end-Effector

The process of deposition is managed by an air-actuated motor which controls the spraying nozzle enabling or disabling the foam deposition. Two tanks containing the Polyol and Isocyanate materials, respectively, are placed in the robotic cell and mixing them together. The polymer foam is then obtained.

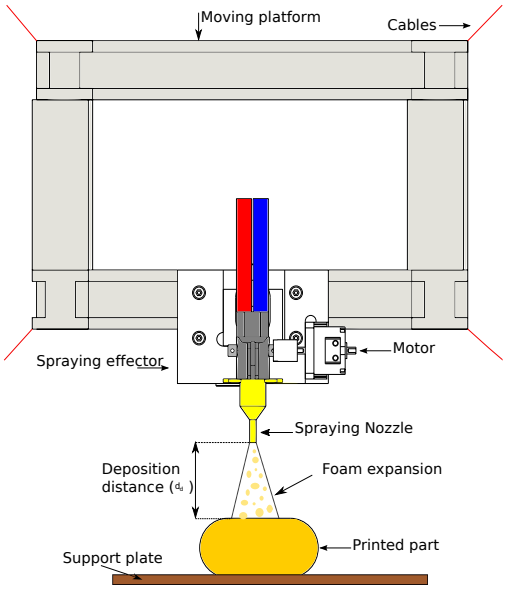

Figure 2. The moving-platform with the spraying gun and its actuation system

The mixture is performed in a static mixer and the compound is then sprayed on the surface of the slab or on the sub-layers as described in Figures 2 and 5. The material expanses and acquires a sufficient stiffness in about six seconds. This time depends on the mix temperature and on the compound reactivity. The foam density is bounded between 35 kg/m^3 and 45 kg/m^3. Its thermal conductivity is equal to 0.027 W.M.K and the Young modulus is equal to 7 MPa. The mean width of the wall created by foam spreading is around 72 mm obtained by adapting different parameters such as flow rates of Isocyanate and Polyol, the distance between the spraying nozzle, the speed of displacement of the nozzle. We now present the robotic architecture i.e. the CDPR which moves the platform.

2.2 CDPR presentation

A CDPR is a robotic system composed of at least 6 cables, reeled in and out by winches, which connect together a frame and a MP. It belongs to a particular class of parallel robots where a MP is linked to a base frame using cables [2][16]. Motors are mounted on a rigid base frame and drive winches. Cable coiled on these winches are routed through exit points located on the rigid frame to anchor points on the MP as shown in Figure 3. By controlling the cable lengths in a synchronous manner, the load can be steadily translated and rotated in a large space with a good dexterity and stability. CDPRs have a large workspace and reach high dynamic performance. Figure 3 depicts the overall architecture of the cable-suspended 3D foam printer with its main components, namely, winches, exit-points and the MP. The winches control the eight cable lengths, which move and actuate the MP. Cables are routed through exit-points located on the rigid frame and connected to anchor-points located on the MP. The printed part is located on the ground so that the MP can access to the top layer of the printed part.

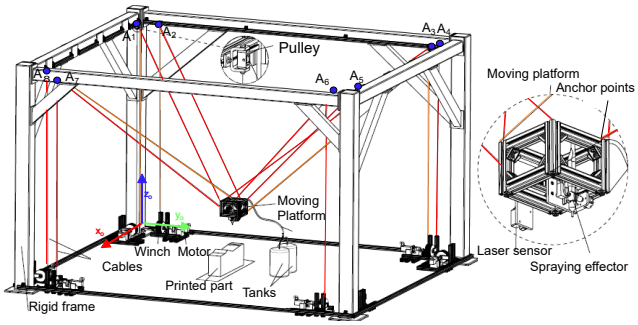

Figure 3. Schematic of a CDPR dedicated to additive foam manufacturing

The extruder is controlled by an output of the controller of the CDPR. The 3D foam printer, named CRAFT and displayed in Figure 4, has the following dimensions: 2.4 m x 3.67 m x 2.76 m (l x b x h). Furthermore, it is reconfigurable and their different reconfiguration strategies were studied in [17], [18], [19].

2.3 Process identification

The maximum possible speed of the flow rate and thus the maximum axial speed of the foam spraying effector is 210 mm/s. This system provides relatively robust position control with a PID position controller and a dynamic positioning error equal to 0.05 mm. An important parameter for printing with the proposed device is the relationship between the spraying nozzle position and the foam flowrate. A model of the foam 3d printing process is expressed in terms of the nozzle height d_d, the velocity of the spray end-effector v_d and the layer height h_c.

The flowrate and the geometrical dimension of the layer were found at different positions and at different deposition speed by measuring on different section of layers. Figure 6 represents the height of foam deposited during a certain

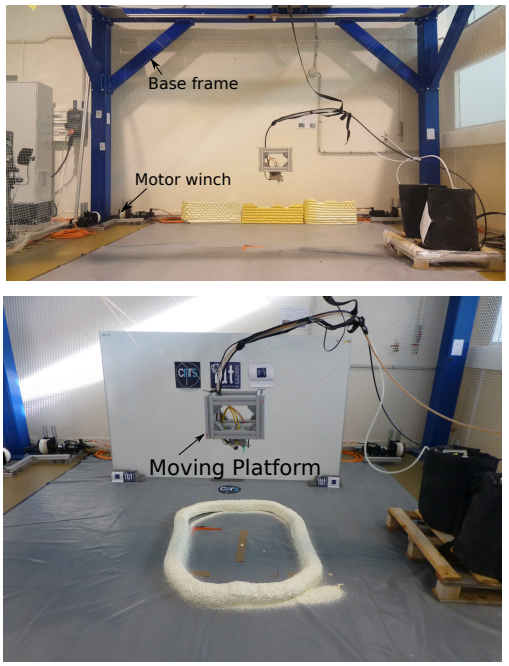

Figure 4. A CDPR, named CRAFT, used for foam additive manufacturing at LS2N, Nantes, France

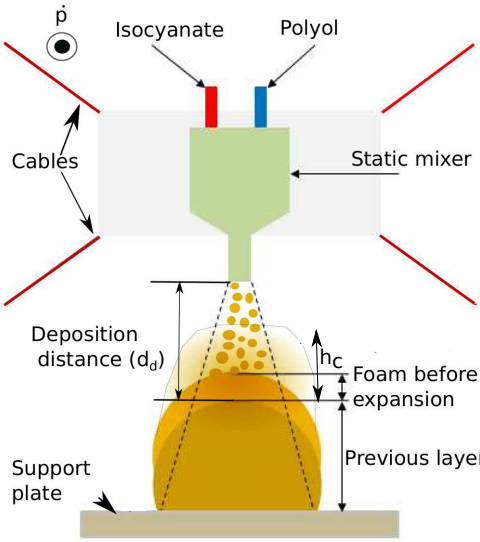

Figure 5. Description of the foam additive manufacturing process and associated variables

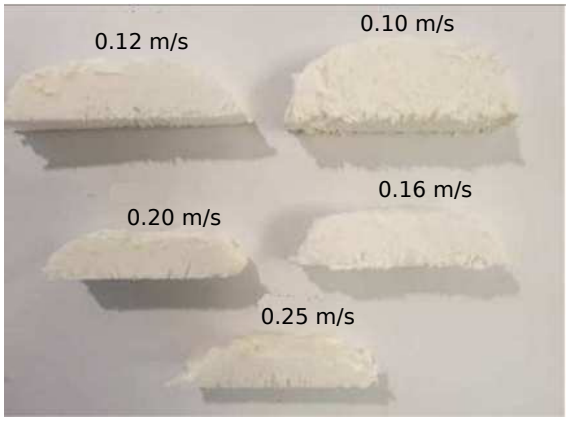

Figure 6. Sectional view of printed foam samples as a function of the linear velocity v_d of the spraying end-effector for deposition distance d_d equal to 150 mm

Table 1. Measured layer height h_c (m)

	d_d (m)		
	0.10	0.15	0.20
0.050	0.071	0.068	0.064
0.075	0.057	0.056	0.045
v_d(m.s^{-1}) 0.100	0.043	0.043	0.034
0.150	0.036	0.027	0.021
0.250	0.024	0.018	0.013

The foam process control model was developed using a non-linear multivariate regression and is illustrated in Figure 7. The blue dots on the response surface are the values obtained from the tests conducted during the identification of the printing process on the CDPR.

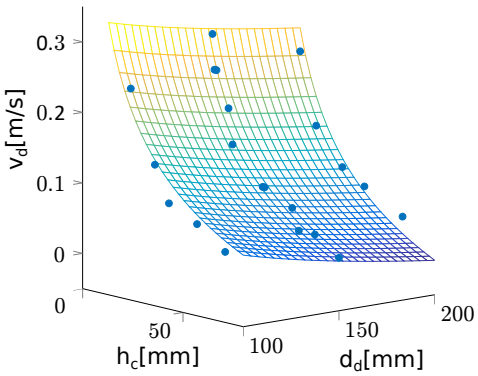

Figure 7. Process modeling characterized by a response surface expressed in Eq.(1) obtained based on a non-linear multivariate regression of data given in Table.1

period of time.

Table 1 gives the measured layer height h_c as a function of v_d and d_d. Figure 7 shows the relationship between the three variables h_c, d_d and v_d governing the foam printing process. It is noteworthy that the printing process under study is non-linear.

The foam printing process is modeled as follows:

$$v_d = b_1 + b_2\, h_c^{b_3} + b_4\, d_d^{b_5} \quad (1)$$

with $b_1 = -1.743$, $b_2 = 1.464$, $b_3 = -0.314$, $b_4 = 1.830$ and $b_5 = -0.054$ being computed with ©Matlab *fitnlm* function from the values given in Tab. 1.

2.4 CDPR Control

The actuators of the CDPR are controlled using a computed torque feed-forward control scheme with a joint space feedback corrector. The integration of the model is performed inside the control law of the CDPR. The control scheme is shown in Fig. 8. The desired velocity of the spray end-effector v_d, namely the one of the moving-platform, along the deposition axis is obtained using Eq. (1). The desired moving-platform twist $\mathbf{t}_d$ is computed by projecting the deposition velocity profile onto the deposition axis. The desired moving-platform pose $\mathbf{x}_d$ and acceleration $\dot{\mathbf{t}}_d$ are obtained using the desired twist first time integrative and derivative respectively. The Inverse Geometric Model (IGM) and the Inverse Kinematic Model (IKM) are used to define the desired joint position $\mathbf{q}_d$ and velocity $\dot{\mathbf{q}}_d$ respectively. Using the measured joint position from the encoder readings, the joint position error $\mathbf{e}_q$ and the joint velocity error $\dot{\mathbf{e}}_q$ are used to define a correction torque $\mathbf{\Gamma}_{PID}$ of the motor in a Proportional Integrative Derivative corrector. A friction compensation torque $\mathbf{\Gamma}_f$ is computed using a viscous and Coulomb friction model with the desired joint velocity to anticipate the actuation torque lost in friction. A feed-forward term accounts for the dynamic and static wrenches exerted on the moving-platform to determine a compensation torque $\mathbf{\Gamma}_{FF}$. The friction compensation torque, the PID corrector torque and the feed-forward torque are summed up to define the actuation torque $\mathbf{\Gamma}$.

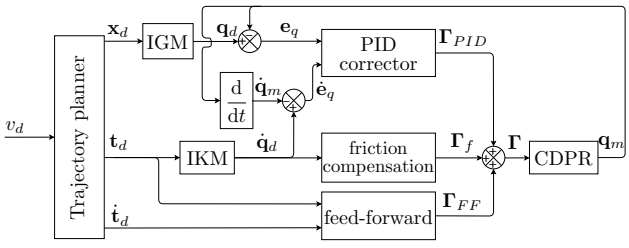

Figure 8. Control scheme of the CDPR used for foam additive manufacturing, the trajectory planner being defined based on the foam additive model (1)

The developed measuring framework is used to improve the flatness surface and achieve the foam process through the implementation of a closed feedback loop. The principle is to keep the geometrical error along the z-axis smaller than 10 mm for one layer thickness. A first approach is to continuously vary the layer thickness proportionally to the measured 'z-error' by using the foam modeling described in Fig 7. This can be achieved either by defining the new operating parameters. It is also possible to adapt the nozzle spraying velocity v_d or to change the deposition height d_d of the nozzle online. The propose framework for foam printing with a CDPR is described in Fig. 9 for a dedicated high dimension parts to be printed. The quality of the foam to be deposited should satisfy some buildability (mechanical characteristics), geometry (shape) and flatness performance. Accordingly, the trajectory to be followed by the spraying end-effector should be defined and well followed.

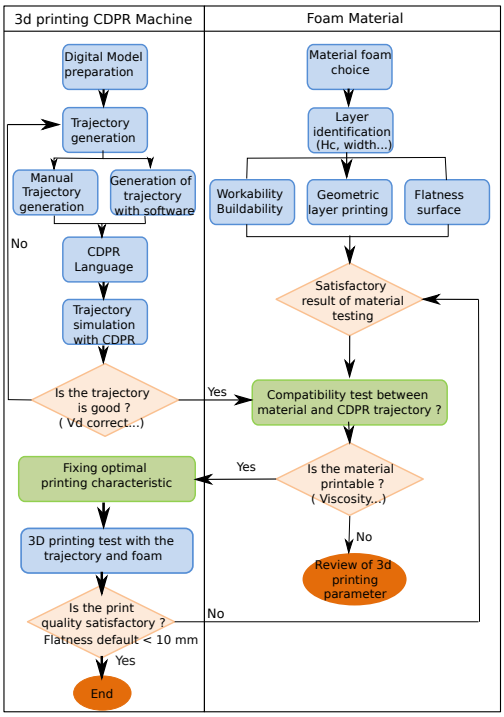

Figure 9. The proposed framework for foam printing with a CDPR

3 Experimental validation

First, some layers were printed using a polyurethane foam with a density of 35kg/m^3. The first tests with the trajectory planner used in the CDPR allowed to test different parameters, in particular the printing speed versus its accuracy. The proposed framework for foam 3D printing with a CDPR is illustrated in Fig 9.

The first tests consisted in printing polylines in order to see the constitution of the robot to follow a straight trajectory, and to test the stacking of the layers. The CDPR well behaved at the tested speeds (up to 0.3m/s) in the

sense that the trajectory remains linear along a line of 1m long and the height d_d remains constant so that the layer thickness is homogeneous at 32 mm, and the layer width is also constant at 70mm (Figure 10 a). After, this experimentation shows a good repeatability of the CDPR trajectories regardless of the printing location in the robot workspace (Figure 10c). We note some widths of non homogeneous layer section, due to the accumulation of material formed at the starting and stopping points of the lines (Figure 10 b).

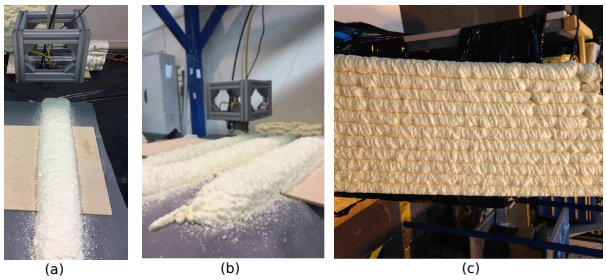

Figure 10. First experimentation polyline printing (a) , polyline with non homonogeneous layer section at the begin and end of layer (b), Layers overlay printing (c)

The second test involved a curved trajectory serving as the pattern for a curved wall. The pattern is 0.8m long and 0.25m wide with the oval shape.

The profile is set to the variables d, e and r, which correspond to the width, length of the profile and the radius of the rounding (see Figure 9) in different frames such as : R_{imp} = (O_{imp}, x_{imp}, y_{imp}, z_{imp}): Printing frame whose origin is the first printing point.
R_{str} = (O_{str}, x_{str}, y_{str}, z_{str}): Structure frame whose origin is the center of the printed structure.
R_p = (O_p, x_p, y_p, z_p): Moving-plateform (MP) frame whose origin is the gravity center of the MP.
R_b = (O_b, x_b, y_b, z_b): Base frame or Global frame related to the fixed frame.

To define the trajectory, the user defines:

- The desired time to move the effector from its initial position (at rest) to the 1st printing point
- The nominal speed of the effector for printing v_{dmax} (which should be kept during printing)
- Number of layers to print
- The height difference between two successive layers

The profile to be printed is defined in R_{imp}. The user places this local coordinate system in the structure frame R_{str} and then in the base reference regarding the robot R_b (Fig.10). To print this experimentation, two types of geometries are used: lines and circular curves. The methodology used for the structure definition is the following :

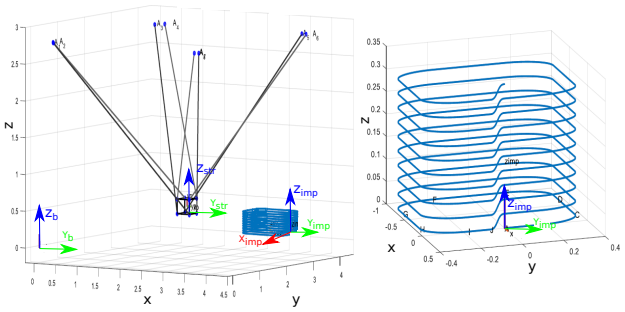

Figure 11. The shape trajectory inside the CDPR Workspace (a) , the printing shape trajectory (b)

- Define the position and orientation of the different frames
- Define the transformation matrixes between the different frames
- Define the shape to be printed in the printing frame R_{imp}
- This shape is first projected in the structure frame R_{str}
- It is then projected in the global frame R_b
- The movement of the moving-platform (MP) is defined by the trajectory.

When the trajectory is defined, the moving platform is suspended in its initial position, which was identified by a laser-tracker. The moving platform goes from the center of the structure frame to the initial printing point. It starts with zero velocity and acceleration and arrives to point A with the desired tracking velocity v_{dmax} (0.3 m/s). The spraying effector based on the moving platform follows the predefined structure shape. There is a vertical transition from one layer to the following. The velocity norm is kept constant, along the printing phase. When printing is finished, the MP goes from the last printed point to the structure center.

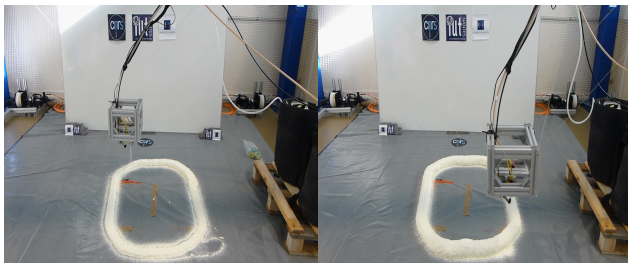

Figure 12. Construction of a foam shape part with the Craft CDPR

The path height and path width used for constructing the shape foam is 70 mm , respectively, the polyurethane foam characteristics. These dimensions were chosen based mainly on the objective to build as large an object as possible, in a reasonable amount of time and the quantity of foam in material tanks. With these dimensions, the shape wall is built in 10 layers and the flatness default is approximately 10 mm. However, other factors include a desire to maximize construction resolution and optimize foam gun performance.

4 Discussion on the results

A prototype system, built at Nantes University, is presented on the CRAFT platform, and data from this system shows its suitability for large-scale printing. In order to scale this out to full-size deployment there are, however, different challenges associated with workspace shape and make correction of flatness surface print are identified as targets for future research. The success of this system demonstrates the feasibility of CDPR for large additive manufacturing systems for construction field.

The proposed novel robotic solution allows the association of the CDPR with a polyarticulated robot, embedded on its mobile platform, on which various end-effectors dedicated to additive manufacturing end-effector based on expanding material, edge finishing tool, measurement/control tool would be mounted (Fig.12).

Many research works have been conducted on the design, modeling and control of CDPR over the last fifteen years because of their numerous potential applications, especially in industry, and their potential improved performances, especially in terms of accuracy. It should be noted that the national platform "XXL Robotics" of the Equipex + TIRREX project (Technological Infrastructure for Robotics Research of Excellence 2021-2028)[1] will be located at LS2N, Nantes University, site Mlab XXL in Saint-Aignan de Grandlieu. This platform will include a reconfigurable cable-driven parallel robot of size 24m x 14m x 6m, equipped with an embedded robotic arm on its moving-platform. This experimental platform will allow us to tackle many industrial applications related to manufacturing robotics and construction robotics such as 3D printing of large parts, namely, adding material, but also removing material such as machining.

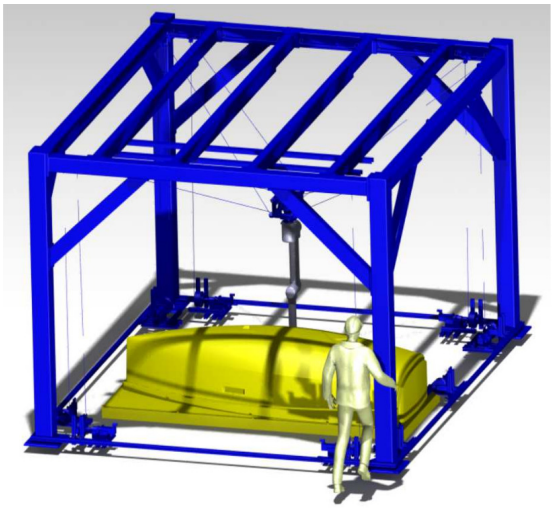

(a)

(b)

Figure 13. (a) Concept of a new CDPR used as a foam large scale printer; (b) reconfigurable CDPR (Nantes University and IRT Jules Verne) used in TIRREX-XXL platform

5 Acknowledgements

This work was supported by the ANR CRAFT project, grant ANR-18-CE10-0004, `https://anr.fr/Project-ANR-18-CE10-0004` and the EquipEx + TIRREX project, grant ANR-21-ESRE-0015.

[1] `https://www.ins2i.cnrs.fr/fr/cnrsinfo/trois-nouvelles-infrastructures-equipex-pour-la-robotique-les-prochaines-semaines`

References

[1] Eric Barnett and Clément Gosselin. Large-scale 3d printing with a cable-suspended robot. Additive Manufacturing, 7:27–44, 2015. jul.

[2] Viktor Mechtcherine, Venkatesh Naidu Nerella, Frank Will, Mathias Näther, Jens Otto, and Martin Krause. Large-scale digital concrete construction–conprint3d concept for on-site, monolithic 3d-printing. Automation in Construction, 107:102933,

2019.

[3] Steven Keating. Towards Site-Specific and Self-Sufficient Robotic Fabrication on Architectural Scales. URL https://www.media.mit.edu/publications/dcp_scirobotics/.

[4] Benoît Furet, Philippe Poullain, and Sébastien Garnier. 3D printing for construction based on a complex wall of polymer-foam and concrete. Additive Manufacturing, 28:58–64, 2019. Num Pages: 7.

[5] Elodie Paquet, Alain Bernard, Benoit Furet, Sébastien Garnier, and Sébastien Le Loch. Foam additive manufacturing technology: main characteristics and experiments for hull mold manufacturing. Rapid Prototyping Journal, 2021.

[6] Jean-Baptiste Izard, Alexandre Dubor, Pierre-Elie Hervé, Edouard Cabay, David Culla, Mariola Rodriguez, and Mikel Barrado. On the improvements of a cable-driven parallel robot for achieving additive manufacturing for construction. In Cable-driven parallel robots, pages 353–363. Springer, 2018.

[7] Julian Kaduk. Development of a computer vision based real-time feedback system for closed-loop control in 3d concrete printing, 2021.

[8] Phillip Chesser. Design of a cable-driven manipulator for large-scale additive manufacturing. 2021.

[9] Chad E. Duty, Vlastimil Kunc, Brett Compton, Brian Post, Donald Erdman, Rachel Smith, Randall Lind, Peter Lloyd, and Lonnie Love. Structure and mechanical behavior of Big Area Additive Manufacturing (BAAM) materials. Rapid Prototyping Journal, 23(1):181–189, January 2017. ISSN 1355-2546. doi:10.1108/RPJ-12-2015-0183. URL https://doi.org/10.1108/RPJ-12-2015-0183.

[10] D Gueners, Helene Chanal, and BC Bouzgarrou. Stiffness optimization of a cable driven parallel robot for additive manufacturing. In 2020 IEEE International Conference on Robotics and Automation (ICRA), pages 843–849. IEEE, 2020.

[11] Edouard Cabay, David Culla, Mariola Rodriguez, and Mikel Barrado. On the improvements of a cable-driven parallel robot for achieving additive manufacturing for construction. In Cable-Driven Parallel Robots: Proceedings of the Third International Conference on Cable-Driven Parallel Robots, volume 53, page 353. Springer, 2017.

[12] Jean-Baptiste Izard, Alexandre Dubor, Pierre-Elie Hervé, Edouard Cabay, David Culla, Mariola Rodriguez, and Mikel Barrado. Large-scale 3d printing with cable-driven parallel robots. Construction Robotics, 1(1):69–76, 2017.

[13] Ishan Chawla, PM Pathak, Leila Notash, AK Samantaray, Qingguo Li, and UK Sharma. Workspace analysis and design of large-scale cable-driven printing robot considering cable mass and mobile platform orientation. Mechanism and Machine Theory, 165: 104426, 2021.

[14] Phillip Chesser, Peter Wang, Joshua Vaughan, Randall Lind, and Brian Post. Kinematics of a cable-driven robotic platform for large-scale additive manufacturing. Journal of Mechanisms and Robotics, pages 1–17, 2021.

[15] Lorenzo Gagliardini, Stéphane Caro, Marc Gouttefarde, and Alexis Girin. Discrete reconfiguration planning for Cable-Driven Parallel Robots. Mechanism and Machine Theory, 100:313–337, 2016. doi:10.1016/j.mechmachtheory.2016.02.014. URL https://hal.archives-ouvertes.fr/hal-01400440.

[16] Damien Gueners, Belhassen-Chedli Bouzgarrou, and Hélène Chanal. Cable behavior influence on cable-driven parallel robots vibrations: experimental characterization and simulation. Journal of Mechanisms and Robotics, 13(4):041003, 2021.

[17] Etienne Picard. Modeling and Robust Control of Cable-Driven Parallel Robots for Industrial Applications. PhD thesis, École centrale de Nantes, 2019.

[18] Zane Zake, Stéphane Caro, Adolfo Suarez Roos, François Chaumette, and Nicolò Pedemonte. Stability analysis of pose-based visual servoing control of cable-driven parallel robots. In International Conference on Cable-Driven Parallel Robots, pages 73–84. Springer, 2019.

[19] Marceau Métillon, Philippe Cardou, Kévin Subrin, Camilo Charron, and Stéphane Caro. A cable-driven parallel robot with full-circle end-effector rotations. Journal of Mechanisms and Robotics, 13(3):031017, 2021.